Specific fibroblastic niches in secondary lymphoid organs orchestrate distinct Notch-regulated immune responses

Nicolas Fasnacht,[1] Hsin-Ying Huang,[2] Ute Koch,[1] Stéphanie Favre,[2] Floriane Auderset,[2,3] Qian Chai,[5] Lucas Onder,[5] Sandra Kallert,[6] Daniel D. Pinschewer,[6] H. Robson MacDonald,[4] Fabienne Tacchini-Cottier,[2,3] Burkhard Ludewig,[5] Sanjiv A. Luther,[2] and Freddy Radtke[1]

[1]Ecole Polytechnique Fédérale de Lausanne, School of Life Sciences, Swiss Experimental Cancer Research, 1015 Lausanne, Switzerland
[2]Department of Biochemistry, [3]WHO Immunology Research and Training Center, and [4]Ludwig Center for Cancer Research, University of Lausanne, 1066 Epalinges, Switzerland
[5]Institute of Immunobiology, Kantonsspital St. Gallen, 9007 St. Gallen, Switzerland
[6]Department of Biomedicine – Haus Petersplatz, Division of Experimental Virology, University of Basel, Petersplatz 10, 4003 Basel, Switzerland

Fibroblast-like cells of secondary lymphoid organs (SLO) are important for tissue architecture. In addition, they regulate lymphocyte compartmentalization through the secretion of chemokines, and participate in the orchestration of appropriate cell–cell interactions required for adaptive immunity. Here, we provide data demonstrating the functional importance of SLO fibroblasts during Notch-mediated lineage specification and immune response. Genetic ablation of the Notch ligand Delta-like (DL)1 identified splenic fibroblasts rather than hematopoietic or endothelial cells as niche cells, allowing Notch 2–driven differentiation of marginal zone B cells and of Esam$^+$ dendritic cells. Moreover, conditional inactivation of DL4 in lymph node fibroblasts resulted in impaired follicular helper T cell differentiation and, consequently, in reduced numbers of germinal center B cells and absence of high-affinity antibodies. Our data demonstrate previously unknown roles for DL ligand-expressing fibroblasts in SLO niches as drivers of multiple Notch-mediated immune differentiation processes.

CORRESPONDENCE
Freddy Radtke:
Freddy.Radtke@epfl.ch
Sanjiv Luther:
sanjiv.luther@unil.ch

Abbreviations used: BEC, blood endothelial cell; BRC, B zone reticular cells; DL, Delta-like; FDC, follicular DC; FRC, fibroblastic reticular cell; GC, germinal center; HEV, high endothelial venule; LEC, lymphatic endothelial cell; LOF, loss-of-function; MRC, marginal reticular cell; MZ, marginal zone; SLO, secondary lymphoid organ; T_{FH}, T follicular helper cell.

Innate and adaptive immune cells in vertebrates are essential to coordinate and promote protective immunity. Primary and secondary lymphoid organs (SLOs) provide special microenvironments allowing development and maturation of immune cells as well as induction and control of immune responses (Junt et al., 2008; Mueller and Germain, 2009). These processes require dynamic interactions between diverse cell populations to trigger the appropriate signals to protect the organism against infections and tumors.

Notch signaling is an evolutionarily conserved cell-to-cell signaling cascade, which in recent years was shown to be importantly involved in lymphocyte development and adaptive immunity (Yuan et al., 2010; Radtke et al., 2013). Vertebrates possess four Notch receptors (N1–N4) that are bound by five different transmembrane ligands of either the Jagged (J1 and J2) or the Δ-like family (DL1, DL3, and DL4). Conditional genetic loss-of-function (LOF) experiments in the mouse revealed that Notch signaling is essential for thymic T cell lineage commitment and maturation (Pui et al., 1999; Radtke et al., 1999), for development of splenic marginal zone (MZ) B cells (Saito et al., 2003; Hozumi et al., 2004) and Esam$^+$ DCs (Skokos and Nussenzweig, 2007; Lewis et al., 2011), as well as for differentiation of follicular helper T cells (T_{FH}) in the LN (Auderset et al., 2013).

The niches and identity of the ligand and/or ligand-expressing cells interacting with the Notch

N. Fasnacht, H.-Y. Huang, and U. Koch contributed equally to this paper.

The Rockefeller University Press $30.00
J. Exp. Med. 2014 Vol. 211 No. 11 2265-2279
www.jem.org/cgi/doi/10.1084/jem.20132528

The Journal of Experimental Medicine

receptor–expressing immune cells are largely unknown. In this regard, thymic T cell development is the notable exception, where DL4-expressing cortical thymic epithelial cells have been identified as niche cells providing Notch-1 signals to developing αβ T cells (Hozumi et al., 2008; Koch et al., 2008).

In the spleen, Notch has been implicated in the development of two important cell types, MZ B cells (Saito et al., 2003; Hozumi et al., 2004) and Esam$^+$ DCs (Skokos and Nussenzweig, 2007; Lewis et al., 2011). MZ B cells mediate the first line of defense against bloodborne pathogens by inducing T cell–independent antibody production. BM transplantation experiments led to the suggestion that the DL1-expressing niche cells for MZ B cell development must be of nonhematopoietic origin (Sheng et al., 2008). As DL1 is highly expressed in blood endothelial cells (BECs) of the red pulp of the spleen, it was hypothesized that they could represent the niche cells driving this process (Tan et al., 2009).

DCs represent a subset of hematopoietic cells that are specialized in antigen presentation. Evidence that Notch signaling is regulating splenic DC development is derived from specific gene inactivation of RBP-J or Notch2 in DCs, which results in a strong reduction of the CD11c$^+$CD8$^-$CD11b$^+$Esam$^+$ subset and a weaker reduction in Esam$^-$ conventional DCs while leaving plasmacytoid DCs largely unaffected (Caton et al., 2007; Lewis et al., 2011). The Esam$^+$ DC subset is involved in priming of CD4$^+$ T cells upon antigen exposure. The ligands and ligand-expressing cells regulating DC development are currently unknown.

Notch signaling has also been implicated in differentiation and function of multiple subsets of T helper cells (Radtke et al., 2013). One recent addition is the role of Notch in T follicular helper (T_{FH}) cell differentiation (Auderset et al., 2013). This is a subset of CD4$^+$ T cells, that differentiates after interactions with DCs and subsequently migrates to the T/B-zone boundary within spleen and LN where they interact with Ag-specific B cells. T_{FH} cells are critically involved in the formation of functional germinal centers (GC), and provide B cell help generating long-lived plasma cells (Crotty, 2011). We recently showed that T cell specific ablation of Notch1 and Notch2 impairs differentiation of T_{FH} cells in draining LNs of mice immunized with T cell–dependent antigens or parasites. Loss of T_{FH} cells in Notch receptor mutant mice impaired GC formation, led to reduced numbers of GC B cells and consequently resulted in the absence of antigen-specific high affinity antibodies (Auderset et al., 2013). The ligands and niche cells responsible for T_{FH} cell differentiation are currently unknown.

Here, we used systematic genetic LOF approaches to identify ligand-expressing niche cells in spleen and LNs, which provide the essential Notch signals for the development of MZ B cells, Esam$^+$ DCs, and T_{FH} cells during T cell–dependent immune responses. Using a recently developed transgenic model (Chai et al., 2013), we refine DL1 expression in the spleen on a subset of stromal CD45$^-$CD31$^-$Pdpn$^-$ cells expressing a Ccl19-Cre transgene (Chai et al., 2013) and show that DL1 deletion in this stromal compartment results in a complete loss of MZ B cells. We describe that the same DL1-expressing stromal cells are responsible for the differentiation of Esam$^+$ DCs. Moreover, we identified DL4-expressing, Ccl19-Cre$^+$ fibroblasts (CD45$^-$CD31$^-$CD35$^{+/-}$Pdpn$^+$) within LNs as important niche cells driving T_{FH} cell differentiation after immunization with T cell–dependent antigens or parasites. Collectively, our data highlight the importance of Notch ligand expressing fibroblasts within SLO for the differentiation of immune cells and T cell dependent antigen-driven immune responses.

RESULTS

MZ B cell development is dependent on DL1-expressing fibroblastic stromal cells of the splenic follicle

It is well accepted that DL1-mediated Notch2 signaling is essential for MZ B cell development. However, how and through which DL1-expressing cell type this lineage decision is instructed is only partially understood. Reconstitution experiments with WT hematopoietic precursors into irradiated DL1-deficient mice have indicated the importance of DL1 expression in radiation-resistant splenic stromal cells rather than in radiation-sensitive hematopoietic cells (Sheng et al., 2008; Tan et al., 2009). Expression analysis of DL1$^{lacZ/+}$ mice identified DL1 expression mostly in BECs present in the red pulp of the spleen suggesting BECs as the likely niche cells for MZ B cell development. To test genetically whether DL1-expressing BECs are, indeed, responsible for MZ B cell differentiation we crossed DL1$^{lox/lox}$ mice with PDGFβ-i$^{CRE\text{-}ERT\text{-}ires\text{-}EGFP}$ mice (Claxton et al., 2008), allowing tamoxifen-induced Cre-mediated inactivation of DL1 in CD31$^+$ endothelial cells (hereafter, called DL1$^{\Delta/\Delta PDGF\beta}$). Immunohistological staining for EGFP confirmed transgenic Cre expression in BECs of the splenic red pulp, as well as in some endothelial cells lining the marginal sinus (Fig. 1 A and not depicted). Genetic inactivation of DL1 was verified by deletion PCR on CD45$^-$Ter119$^-$CD31$^+$ cells sorted from splenic digests (Fig. 1 B). Surprisingly, relative and absolute numbers of MZ B cells were not significantly altered in DL1$^{\Delta/\Delta PDGF\beta}$ mice compared with control animals 2 mo after gene inactivation (Fig. 1, C and D). These genetic data suggest DL1-expressing BECs are not the essential niche cells for MZ B cell fate specification.

Because Delta ligands have been reported to be expressed on DCs (Skokos and Nussenzweig, 2007; Sekine et al., 2009), we also intercrossed DL1$^{lox/lox}$ mice with CD11c-Cre mice (DL1$^{\Delta/\Delta CD11c}$) to formally exclude that some potentially radiation-resistant DC subset might function as niche cells for MZ B cell development. However, MZ B cell development was unperturbed in DL1$^{\Delta/\Delta CD11c}$ mice compared with controls (Fig. 1 E and not depicted). These inherently negative results, together with the previously reported data using chimeric mice (Sheng et al., 2008; Tan et al., 2009), excluded BECs and hematopoietic cells (including DCs) from being the critical DL1-expressing cells for MZ B cell development.

We therefore hypothesized that mesenchymal stromal cells of the spleen could be part of the DL1-expressing niche for MZB development. To test this possibility, we made use of

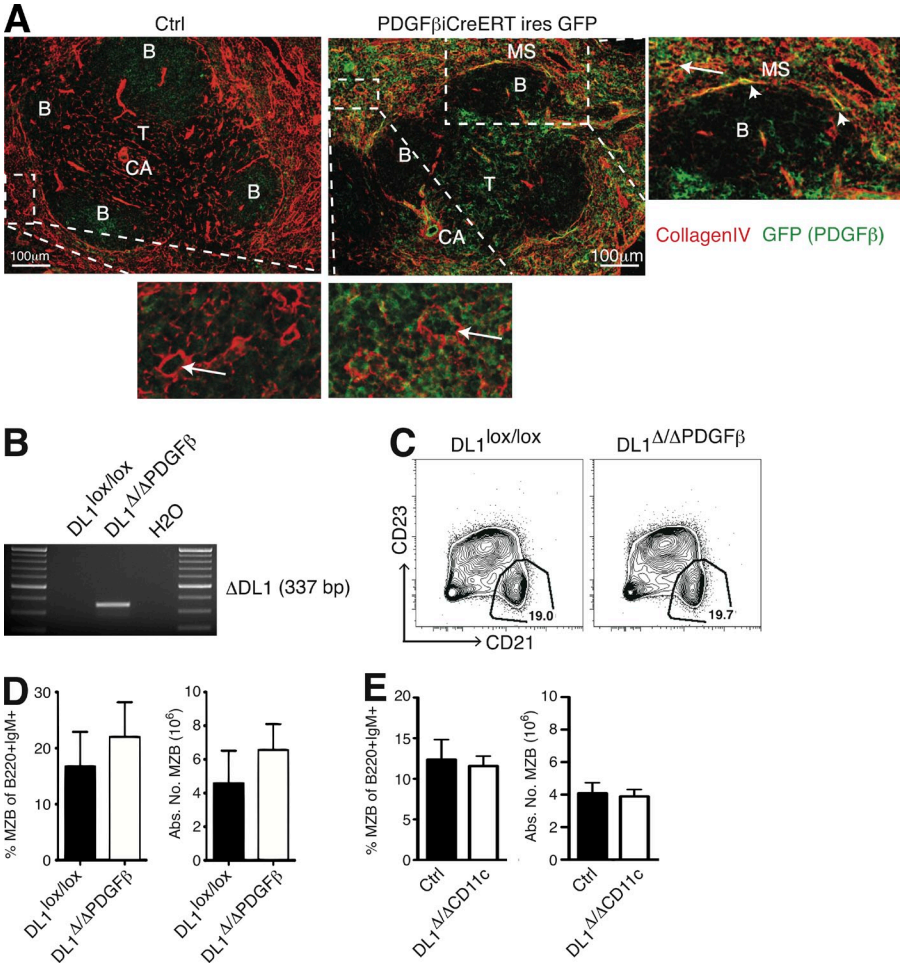

Figure 1. Inactivation of DL1 in PDGFβ$^+$ BECs or CD11c$^+$ DCs does not perturb MZ B cell development. (A) Spleen sections of control (DL1$^{lox/lox}$) and induced DL1^{PDGFβiCreERT} mice were stained for Collagen IV and GFP. Collagen IV stains basement membranes, most notably around blood vessels and in the marginal sinus. GFP is expressed bicistronically by the PDGFβ-promoter transgene construct. The dashed boxes are represented as a higher magnification on the right or below. B, B cell follicle; T, T cell zone; CA, central arteriole; MS, marginal sinus. Arrows indicate BECs and arrowheads the marginal sinus. (B) DL1 deletion PCR on sorted CD45$^-$Ter119$^-$CD31$^+$ endothelial cells from spleens of control and tamoxifen-injected DL1$^{Δ/ΔPDGFβ}$ mice. (C) Representative flow cytometry profile of MZ B cells (gated as CD21^{hi}CD23^{int}), pregated on B220$^+$IgM^{hi} cells, in spleens of control and tamoxifen-injected DL1$^{Δ/ΔPDGFβ}$ mice. (D) Bar diagrams show relative (left) and absolute cell number (right) of MZ B cells (MZB) in spleens of control and TAM-injected DL1$^{Δ/ΔPDGFβ}$ mice (means ± SD of 4–5 animals per group). One of two representative experiments is shown. (E) Bar diagrams show relative (left) and absolute number (right) of splenic MZ B cells of control and DL1$^{Δ/ΔCD11c}$ mice (means ± SD of 4–5 animals per group).

a BAC transgenic mouse model that drives expression of the Cre recombinase under the control of the Ccl19 promoter (Ccl19-Cre) that is known to be active in fibroblastic reticular cells (FRC) of the T zone (Onder et al., 2011; Chai et al., 2013). We intercrossed DL1$^{lox/lox}$ and DL4$^{lox/lox}$ mice with the BAC transgenic-cre driver line and generated DL1$^{lox/lox}$ Ccl19-Cre and DL4$^{lox/lox}$ Ccl19-Cre, hereafter called DL1$^{Δ/ΔCcl19}$ and DL4$^{Δ/ΔCcl19}$, respectively. Littermates lacking the Cre transgene were used as negative controls.

Flow cytometric analysis of splenic B cells derived from DL1$^{Δ/ΔCcl19}$ mice revealed a complete loss of MZ B cells, whereas inactivation of only one DL1 allele resulted in an ∼50% reduction in relative and absolute MZ B cell numbers (Fig. 2, A and B). As expected, inactivation of DL4 in splenic stromal cells using DL4$^{Δ/ΔCcl19}$ mice had no effect on MZ B cell frequencies (not shown). These mice were analyzed as negative control to ensure that Ccl19-Cre expression does not perturb MZ B cell development. Immunohistological analysis of spleen sections confirmed loss of IgM$^+$ IgD$^-$ MZ B cells localizing just adjacent to the laminin$^+$ marginal sinus in DL1$^{Δ/ΔCcl19}$ but not in control animals (Fig. 2 C).

To exclude a possible contribution of hematopoietic cells that may express Ccl19-Cre, we generated reverse chimeras. CD45.2$^+$ DL1$^{lox/lox}$, DL1$^{+/ΔCcl19}$ and DL1$^{Δ/ΔCcl19}$ mice were lethally irradiated and subsequently reconstituted with CD45.1$^+$ WT BM cells. Reconstitution efficiency 12 wk after transplantation was >85% (unpublished data). DL1$^{+/ΔCcl19}$ and DL1$^{Δ/ΔCcl19}$ reverse BM chimeras revealed a dose-dependent reduction of MZ B cell numbers (Fig. 2, D and E). Collectively, these results demonstrate that Ccl19-Cre–expressing splenic stromal cells are the essential DL1$^+$ cells for Notch2 driven MZ B cell development.

To characterize these splenic stromal niche cells, we intercrossed Ccl19-Cre with R26-EYFP and R26R^{mTmG} reporter mice. In these mice, Cre-mediated excision of the lox-stop-lox cassette triggers EYFP or GFP expression only in Ccl19-expressing cells. Initially, R26-EYFP x Ccl19Cre mice were investigated and EYFP expression was predominantly found in a reticular pattern throughout the white pulp of the spleen, including Pdpn$^+$ T zone FRCs (Fig. 3 A), as expected (Chai et al., 2013). Besides confirming Cre-mediated EYFP expression in T zone FRCs, immunohistological analysis of the spleen also identified EYFP expression in three follicular fibroblast populations: follicular DCs (FDCs), MAdCAM-1$^+$ marginal reticular cells (MRCs) below the collagen IV$^+$ subcapsular sinus, and reticular cells of the outer follicle,

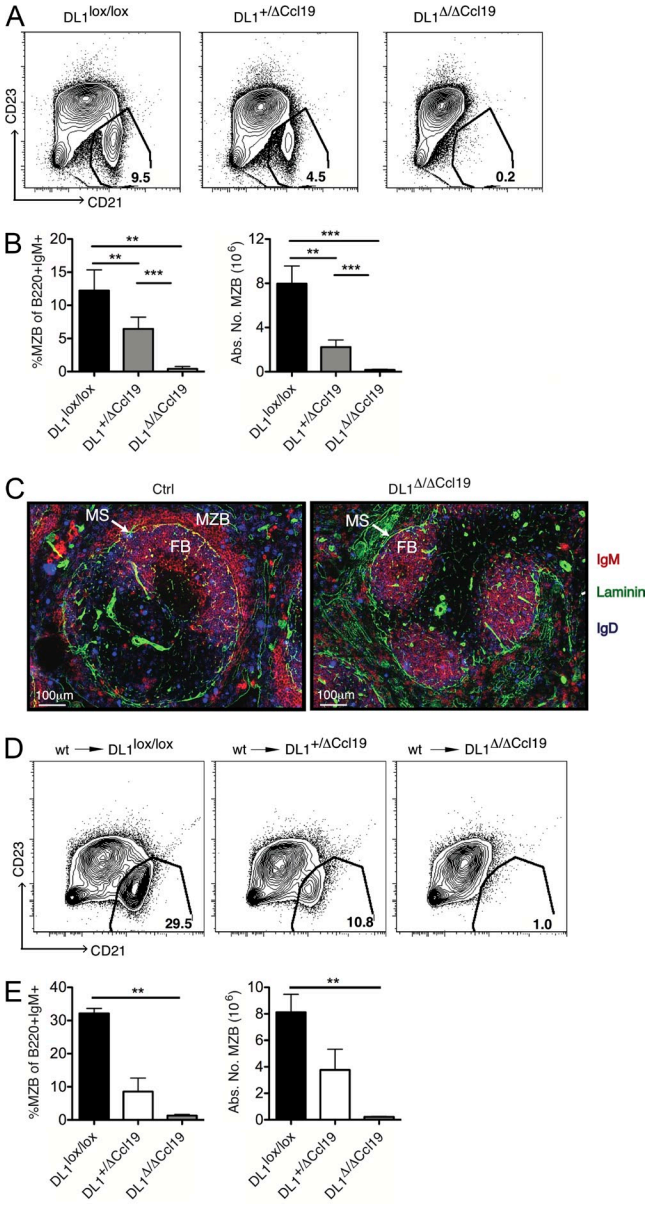

Figure 2. DL1-expressing Ccl19-Cre$^+$ splenic stromal cells are the essential niche cells for MZ B cell differentiation. (A) Representative FACS profile displaying the frequency of splenic MZ B cells (gated as CD21^{hi}CD23^{int}) among B220$^+$IgM^{hi} cells in control, DL1$^{+/\Delta Ccl19}$, and DL1$^{\Delta/\Delta Ccl19}$ mice. (B) Bar diagrams show relative (left) and absolute numbers (right) of splenic MZ B cells (means ± SD of 5–6 animals per group). (C) Spleen sections of control and DL1$^{\Delta/\Delta Ccl19}$ mice were stained for IgM, IgD, and Laminin, as indicated. MS, marginal sinus (laminin$^+$); FB, follicular B cells (IgM$^+$D$^+$); MZB, MZ B cells (IgM$^+$D$^-$). (D) Representative FACS profiles displaying the frequency of splenic MZ B cells (CD21^{hi}CD23^{int}) among B220$^+$IgM^{hi} cells in control, DL1$^{+/\Delta Ccl19}$ and DL1$^{\Delta/\Delta Ccl19}$ reverse BM chimeras. (E) Bar diagrams show relative (left) and absolute numbers (right) of splenic MZ B cells in the reverse BM chimeras (means ± SD of 6–7 animals per group). **, P < 0.01; ***, P < 0.001. Unpaired Student's *t* test was used to determine significance. Results are a composite of three independent experiments.

referred here as B zone reticular cells (BRC; Fig. 3 A and not depicted).

To characterize the various splenic stromal cell populations, an isolation and gating strategy was established that allows the identification of three stromal cell subsets by flow cytometry: Pdpn$^+$CD31$^-$ FRC, Pdpn$^-$CD31$^+$ BECs, and Pdpn$^-$CD31$^-$ cells (double negative; DN). The gating on GFP$^+$ cells in Ccl19-Cre reporter mice also allows the exclusion of most red pulp fibroblasts. Ccl-19 Cre-triggered GFP expression in another comparable R26R^{mTmG} reporter strain was found in a small subset of splenic stromal cells, with the vast majority of GFP$^+$ cells belonging to T zone FRC and DN cells with the former population being markedly enriched over the nondeleted Tomato-expressing cells (Fig. 3 B; Chai et al., 2013). DN cells are likely to include all three follicular fibroblast subsets (FDCs, MRCs, and BRCs), in addition to most red pulp fibroblasts. Importantly, BECs showed hardly any deletion, which is consistent with histological findings. No GFP expression was observed in hematopoietic cells, including DCs (unpublished data). Comparable results were obtained using the previously used reporter strain, R26^{EYFP} (unpublished data). Ccl19-cre x R26R^{mTmG} were also crossed onto the DL1$^{lox/lox}$ background to investigate DL1 gene deletion in the GFP$^+$ spleen stroma subsets. Five clearly detectable stromal cell populations were sorted based on Tomato (Ccl19-Cre inactive) or GFP (Ccl19-Cre active) expression with DL1 deletion being confined to a subpopulation of GFP$^+$ cells of the FRC and DN type (Fig. 3 C). Although only a partial DL1 deletion could be detected in GFP$^+$ cells, a complete loss of MZ B cells was observed in DL1$^{\Delta/\Delta Ccl19}$ mice (Fig. 2 A). These results suggest that the Rosa gene locus is more accessible to Cre-mediated deletion compared with the DL1 locus and/or that DL1 is only expressed in a subset of GFP$^+$ FRC or DN cells.

Next, we assessed DL1 expression in various stromal subsets to further characterize the niche cell. As DL1 protein expression could not be reproducibly detected on the surface of isolated stromal and hematopoietic cells, these cells were sorted from digested spleens of R26R^{mTmG} x Ccl19-Cre mice and analyzed for DL1 transcripts by qRT-PCR. These experiments revealed a strong enrichment of DL1 transcripts in GFP$^+$ DN cells relative to Tomato$^+$ DN cells (Fig. 3 D) consistent with the notion that GFP identifies a DN fibroblast subset largely restricted to the white pulp cord, whereas Tomato$^+$ DN cells are likely to be enriched in red pulp fibroblasts. FRC, BECs, and meshed splenocytes showed much lower DL1 transcript levels. Comparable DL1 expression was observed with cells sorted from the spleen of R26-EYFP x Ccl19-Cre reporter mice (unpublished data). In contrast, in both mouse strains DL4 expression was predominantly confined to the Ccl19-Cre$^-$ FRC subset, whereas both Tomato$^+$ and GFP$^+$ FRC subsets expressed Pdpn transcripts (unpublished data).

DL1 expression and inactivation was further investigated by immunohistochemistry on spleen sections derived from

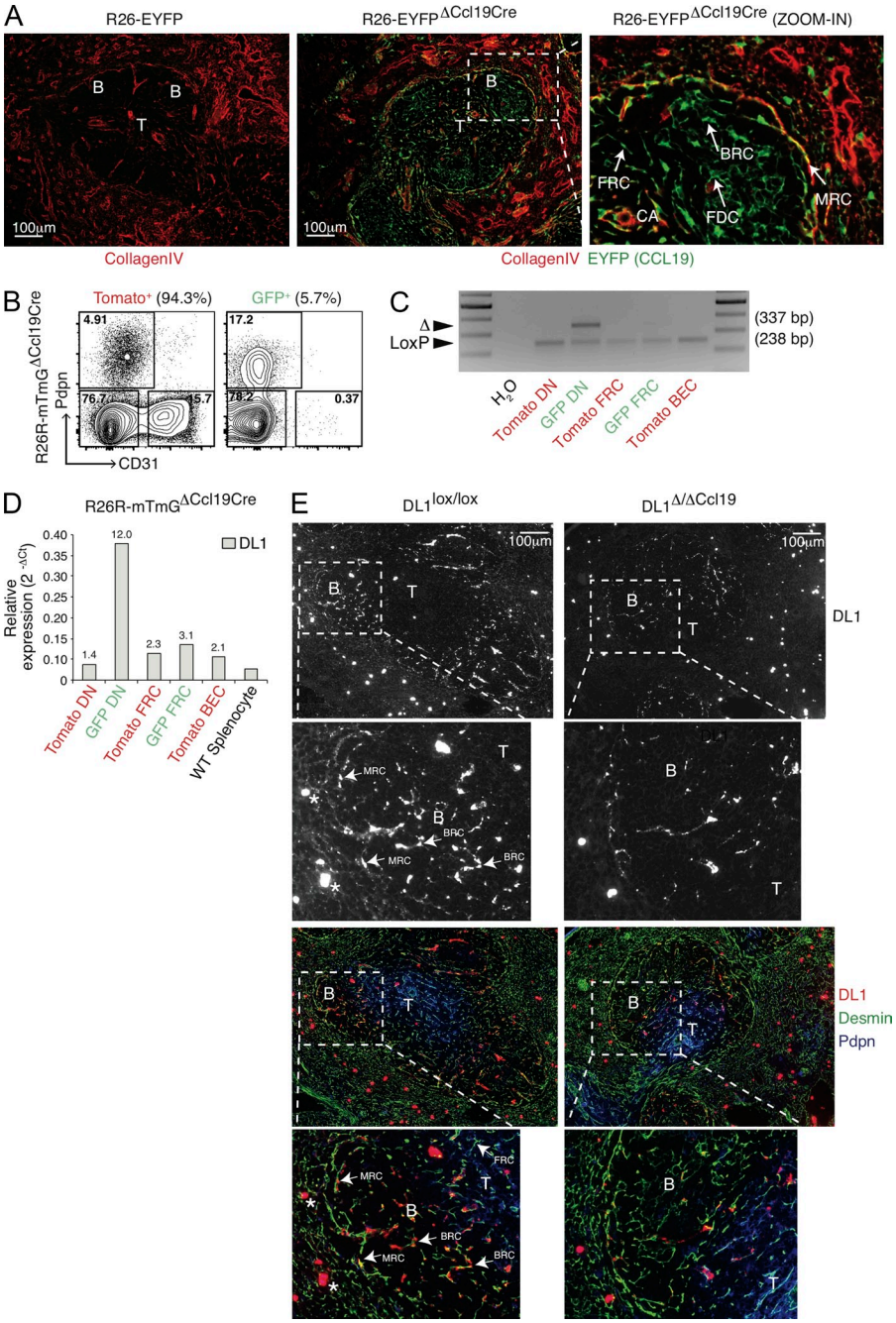

Figure 3. Characterization of Ccl19-Cre activity and DL1 expression in stromal cells of the spleen. (A) Spleen sections of R26-EYFP (control) and R26-EYFP$^{\Delta Ccl19}$ mice stained for EYFP and collagen IV expression. EYFP staining is indicative for Cre recombinase activity through the deletion of the lox-stop-lox cassette in the R26 gene locus. Collagen IV highlights the basement membrane of blood vessels and the marginal sinus. The dashed box is represented as a higher magnification on the right side. B, B cell follicle; T, T cell zone. Arrow head pointing to EYFP reticular cells. FDCs; MRC, marginal fibroblastic reticular cells; BRCs; FRC, T zone fibroblastic reticular cells; CA, central arteriole. (B) Representative FACS profile of Tomato$^+$ (Ccl19-Cre$^-$) and GFP$^+$(Ccl19-Cre$^+$) splenic stromal cells isolated from mTmG$^{\Delta/+Ccl19}$ reporter mice gated on Aqua$^-$Ter119$^-$CD45$^-$CD35$^-$ cells and further analyzed for the expression of podoplanin (Pdpn, gp38$^+$) and CD31. GFP$^+$ cells represent the fraction of cells that express Ccl19-Cre. Percentages indicate the mean frequency among CD35$^-$ stromal cells (n = 5). (C and D) Cell populations from digested spleens of three individual mTmG$^{\Delta/+Ccl19}$ mice were sorted as indicated in B, pooled, and assessed by semiquantitative PCR for the deleted (Δ) versus undeleted (loxP) DL1 gene (C) and by qRT-PCR for relative mRNA expression levels (D). The numbers in D indicate the fold enrichment relative to total WT splenocytes. Bars in D represent data from triplicate PCR reactions normalized to the HPRT housekeeping gene of pooled sorted stromal cells from 3 individual mice for the indicated reporter line. (E) Splenic sections of DL1$^{lox/lox}$ and DL1$^{\Delta/\Delta Ccl19}$ mice were stained for DL1 (top), Pdpn, and desmin (bottom) as indicated. Arrows point to different sites of DL1 expression and stars denote examples of background staining (in form of larger dots) due to endogenous horseradish peroxidase activity. The dashed boxes are represented as a higher magnifications shown below the images. Experiments shown in A, B, and E are representative of two to five experiments with at least three different mice per group.

control and DL1$^{\Delta/\Delta Ccl19}$ mice (Fig. 3 E). Histologically, DL1 expression was found in several desmin^{high} cell types, including MRCs, BRCs surrounding the desmin^{low} CD35$^+$ FDC cluster, and Pdpn$^+$ FRC in the outer but not central T zone (Fig. 3 E). Surprisingly, DL1 expression was not detectable within the MZ or on red pulp vessels. Given that MRC and BRC of the spleen lack Pdpn and CD31 expression, they should be comprised in the DL1-transcript expressing DN cells identified by flow cytometry (Fig. 3, B–E).

DL1-expressing stromal cells are required for development of splenic Esam$^+$ DCs

DC-specific genetic LOF studies for RBP-J and Notch2 have revealed important functions of canonical Notch signaling for the development and homeostasis of specific subsets of splenic DCs. RBP-J is essential for the generation of CD8$^-$CD11b$^+$Esam$^+$ DCs, whereas Notch2 receptor signaling was implicated in the generation of all cDC types, including CD8$^-$, CD8$^+$ and CD11b$^+$ DC subsets (Caton et al., 2007;

Lewis et al., 2011). The Notch ligand responsible for directing splenic DC development is currently unknown. Because Esam$^+$ DCs have been shown to be Notch2 dependent (Lewis et al., 2011), similar to MZ B cells, and to localize close to the splenic MZ (Caton et al., 2007), we hypothesized that both cell lineages might be specified by the same DL1-expressing stromal cells. To test this hypothesis, we analyzed the splenic DC compartment of DL1$^{\Delta/\Delta Ccl19}$ compared with control animals. Loss of DL1 resulted in a marked decrease in relative and absolute numbers of CD11c$^+$ DCs (Fig. 4, A and B). CD8$^-$Esam$^+$ DCs are the most affected DC type but also splenic CD8$^+$ and CD11b$^+$ DC subsets showed lower overall percentages and absolute cell numbers in DL1$^{\Delta/\Delta Ccl19}$ compared with control mice (Fig. 4, C and D). In contrast to MZ B cell development, where loss of one DL1 allele resulted in a 50% reduction of MZ B cell numbers, the development of DL1-induced DCs appeared not to depend on ligand dosage (Fig. 4, A–D). As expected, deletion of DL4 in Ccl19-Cre$^+$ cells did not lead to significant changes in any of the DC subsets analyzed, thereby demonstrating that only DL1 is essential for DC development (unpublished data). To exclude the possibility that splenic DC development is perturbed due to inappropriate inactivation of DL1 in a small subset of hematopoietic cells, reverse chimeras (WT→DL1$^{\Delta/\Delta Ccl19}$, WT→DL1$^{+/\Delta Ccl19}$, and WT→DL1$^{lox/lox}$) were generated and analyzed 12 wk after transplantation. The results of the reverse chimeras (unpublished data) confirmed and were consistent with the observations in the DL1$^{\Delta/\Delta Ccl19}$ mutant animals, indicating that loss of DL1 in stromal cells of the spleen is causative for the reduction of specific splenic DC subsets.

Esam$^+$ DCs have been shown to be critical for priming of CD4$^+$ T cells (Lewis et al., 2011). To test whether CD4

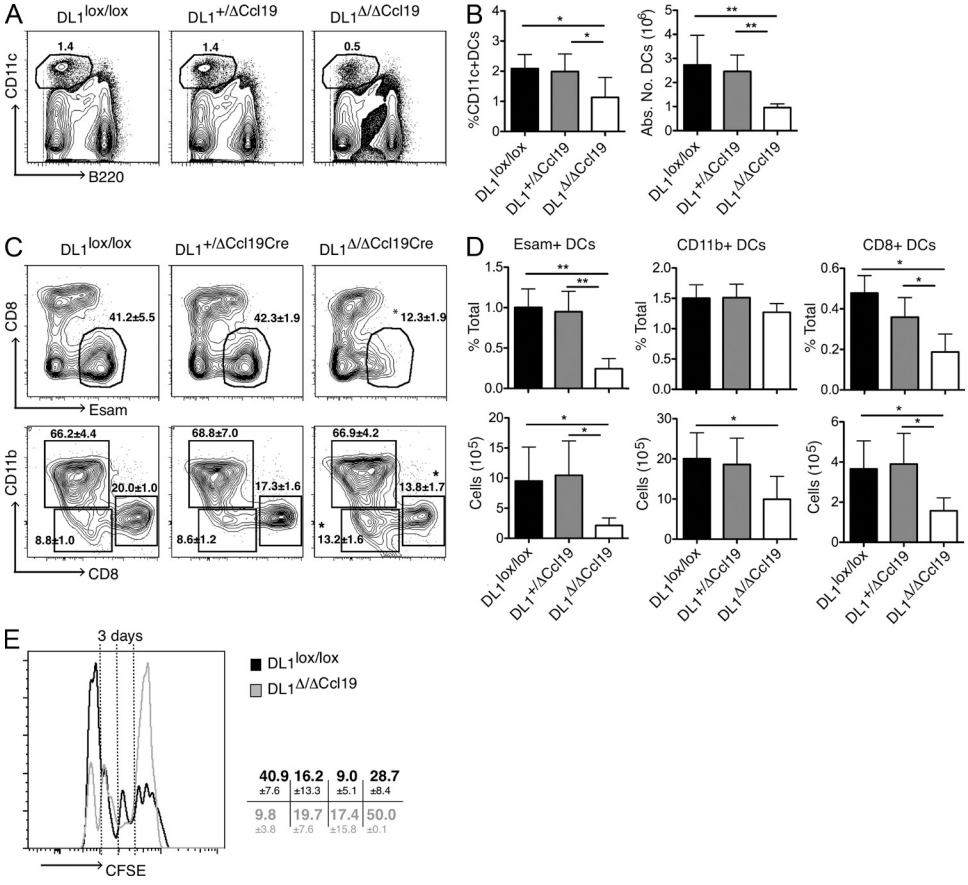

Figure 4. DL1-expressing Ccl19$^+$ splenic stromal cells regulate Notch-mediated differentiation of Esam$^+$ DCs. (A) Representative FACS profile of splenic DCs (gated as CD11c$^+$B220$^-$) of control, DL1$^{+/\Delta Ccl19}$ and DL1$^{\Delta/\Delta Ccl19}$ mice. (B) Bar diagrams show relative (left) and absolute numbers (right) of total splenic DCs (means of 4–5 mice per group, of two independent experiments). (C) Representative FACS profiles of Esam expression on total splenic CD11c$^+$ DCs (top) and the different DC subsets (bottom), classified with CD8α and CD11b expression. Percentages represent mean ± SD of 5 animals per group of two independent experiments. (D) Bar diagrams show relative (top) and absolute numbers (bottom) of Esam$^+$, CD11b$^+$, and CD8α$^+$ DCs from spleens of control, DL1$^{+/\Delta Ccl19}$ and DL1$^{\Delta/\Delta Ccl19}$ mice (mean ± SD of 4–5 animals per group of two independent). (E) In vivo priming of CD4$^+$ T cells in absence of Esam$^+$ DCs. OT-II CD4$^+$ T cells were purified, labeled with CFSE, and injected i.v. into control and DL1$^{\Delta/\Delta Ccl19}$ mice that were subsequently immunized with OVA and LPS as adjuvant. 3 d later, splenic cells were analyzed for the proliferation of the CFSE-labeled OT-II T cells. Representative data of one experiment are depicted and percentages of each cell division are shown as mean ± SD of two independent experiments with at least three animals per group. *, $P < 0.05$; **, $P < 0.01$. Unpaired Student's *t* test was used to determine significance.

T cell priming is affected in DL1 mutant animals, ovalbumin-specific OT-II $CD4^+$ T cells were transferred into $DL1^{\Delta/\Delta Ccl19}$ or control mice, and subsequently immunized with OVA and LPS as adjuvant. Although OT-II $CD4^+$ T cells were primed by wild-type DCs and therefore proliferated, $CD4^+$ T cell priming in $DL1^{\Delta/\Delta Ccl19}$ mice was strongly reduced correlating with the severe reduction of $Esam^+$ DCs and other DC subtypes (Fig. 4 E). Collectively, these data identify DL1 as the ligand responsible for DC development in the spleen, most notably for $Esam^+$ DCs in the MZ. Moreover, they reinforce the importance of Ccl19-cre^+ DL1-expressing fibroblasts in instructing Notch-2 dependent development not only of MZ B cells but also of splenic DC.

DL4-expressing stromal cells of the LN are important niche cells for T follicular helper cell and GC B cell differentiation

We recently reported that Notch signaling regulates follicular T helper cell (T_{FH}) differentiation (Auderset et al., 2013). T cell–specific gene ablation of Notch1 and Notch2 impaired differentiation of T_{FH} cells in draining LNs of mice immunized with T cell–dependent antigens and parasites. Impaired T_{FH} cell differentiation correlated with deficient GC development and absence of high-affinity antibodies (Auderset et al., 2013). The ligands and ligand-expressing cells involved in this process are currently unknown. To identify the hematopoietic-specific ligands that may trigger Notch-induced T_{FH} cell differentiation, we made use of Mx-Cre mice and generated BM chimeras transplanting $CD45.2^+$ BM cells from poly I-C–induced $DL1^{\Delta/\Delta Mx}$, $DL4^{\Delta/\Delta Mx}$, $DL1/DL4^{\Delta/\Delta Mx}$, $J1^{\Delta/\Delta Mx}$, $J2^{\Delta/\Delta Mx}$, and $J1/J2^{\Delta/\Delta Mx}$ mice into lethally irradiated $CD45.1^+$ wild-type mice. 12 wk after transplantation reconstitution efficiency for all BM chimeras was >90% (unpublished data). The different chimeric mutant and control animal cohorts were then immunized with NP-CGG in alum and analyzed 14 d after immunization for the presence of $PD1^+CXCR5^+$ T_{FH}, $B220^+GL7^+CD95^+$ GC B cells and for high affinity NP-specific antibodies. Surprisingly, T_{FH} cells, GC B cells and high-affinity antibodies developed normally in the various BM chimeras tested (unpublished data). To exclude the possibility that these inherently negative results are simply a consequence of the chosen antigen, we repeated the experiments using *Schistosoma mansoni* eggs as a second independent model of immunization. *S. mansoni* eggs induce a stronger Th2 immune response and T_{FH} cell differentiation. However the results of this immunization protocol were similar to and in agreement with the NP-CGG model. T_{FH} cells, GC B cells, *S. mansoni* soluble egg antigens (SEA)-specific antibodies were comparable between control and DL mutant BM chimeras (unpublished data). Inefficient inactivation of DL1 and DL4 or insufficient reconstitution of the different BM chimeras were excluded as possible reasons for these negative results (unpublished data). Collectively, these data strongly suggest that expression of Notch ligands on hematopoietic cells is dispensable for the generation of T_{FH} cells.

Having shown the importance of DL1-expressing stromal cells in the spleen for the specification of MZ B cells and certain DC subsets, we now explored whether such a mechanism could be conserved between different SLO. Therefore, we investigated if Ccl19-Cre^+ LN stromal cells could be the ligand-expressing niche cells that influence T_{FH} differentiation. To investigate whether LN stromal cells might play a role in mediating Notch signals, Notch ligand mRNA expression was assessed on sorted stromal subpopulations based on CD31 and Pdpn expression before, and two and five days after NP-CGG immunization. Because DL1 and DL4 mRNA expression was up-regulated in $Pdpn^+$ and in $CD31^+$ cells after immunization (unpublished data), we focused our analysis on using DL1 and DL4 mutant animals that were crossed to Ccl19-Cre mice. $DL1^{\Delta/\Delta Ccl19}$ and $DL4^{\Delta/\Delta Ccl19}$ were analyzed 14 d after NP-CGG immunization. Although Ccl19-Cre-mediated inactivation of DL1 did not affect T_{FH} cells, GC B cells or the production of NP-specific antibodies, $DL4^{\Delta/\Delta Ccl19}$ mice exhibited a severe reduction in $CD4^+CXCR5^+PD1^+$ T_{FH} cells and concomitantly in GC B cells (Fig. 5, A and B). Both total and high affinity NP-specific antibodies were also drastically reduced in sera of $DL4^{\Delta/\Delta Ccl19}$ but not $DL1^{\Delta/\Delta Ccl19}$ or control animals (Fig. 5 C). Interestingly, reduction in T_{FH} and GC B cells was similar in $DL1/DL4^{\Delta/\Delta Ccl19}$ and $DL4^{\Delta/\Delta Ccl19}$ mice indicating that DL1 cannot compensate for DL4 deficiency (Fig. 5, A–C). Immunization of the same DL mutant and control animals with *S. mansoni* eggs as second independent model confirmed the important role of DL4-expressing LN stromal cells as inducers of T_{FH} and GC B cell differentiation, and of high affinity antibody responses following immunization with T-dependent antigens (Fig. 5, D–F).

To further characterize these Ccl19-Cre^+ LN stromal niche cells we analyzed R26-EYFP $^{\Delta Ccl19Cre}$ reporter mice 5 d after NP-CGG immunization. Immunohistological analysis for the expression of EYFP was combined with the FDC marker CD35 and Pdpn, which is predominantly expressed on T zone FRCs but also on activated FDCs. Cre-mediated activity was observed in three fibroblast populations: $CD35^+Pdpn^+$ FDCs and $CD35^-Pdpn^+$ cells with the latter comprising T zone FRCs, MAdCAM-1^+ MRCs and some BRCs (Fig. 6 A; not depicted).

To further study DL4-expressing stromal cells, an improved isolation protocol was established allowing not only the better isolation and identification of FRC, lymphatic endothelial cells (LECs) and BECs, as described previously (Link et al., 2007), but also of $CD35^+Pdpn^+$ FDC. The finding that the isolated FDC express high levels of both CD35 and CD157 (BP3; Fig. 6 B, C) and were virtually absent in B cell deficient mice (unpublished data) suggested that we had successfully isolated and stained FDC from LN of WT mice. Flow cytometric analysis of stromal cells from LN of control and $DL4^{\Delta/\Delta Ccl19}$ mice largely confirms the immunohistochemical analysis as it reveals that activated FDC ($CD35^+$ $CD31^-Pdpn^+$) shows the highest surface DL4 expression, which is abolished by Ccl19-Cre–mediated deletion, followed by FRC (CD35-$CD31^-Pdpn^+$) and to a lesser extent LEC ($CD35^-CD31^+Pdpn^+$; Fig. 6 B). While transcripts for DL4 were observed to be enriched in several stromal cell

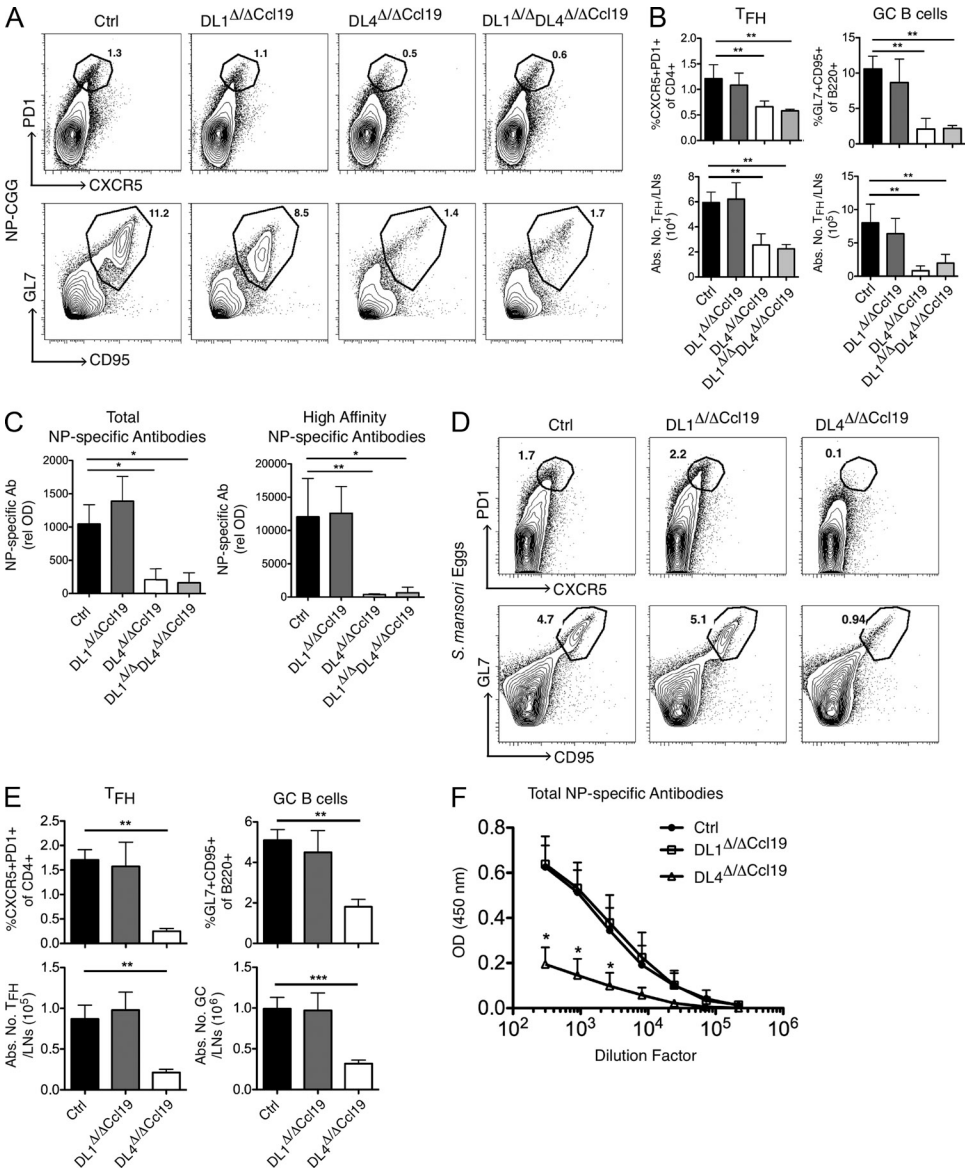

Figure 5. DL4 expression on Ccl19$^+$ LN fibroblasts is required for T_{FH} and GC differentiation. (A) Representative FACS profiles of CD4$^+$CXCR5$^+$PD1$^+$ T_{FH} cells (top) and GL7$^+$CD95$^+$ GC B cells (bottom) from control, DL1$^{\Delta/\Delta Ccl19}$, DL4$^{\Delta/\Delta Ccl19}$, and DL1$^{\Delta/\Delta}$DL4$^{\Delta/\Delta Ccl19}$ mice 14 d after immunization with NP-CGG. Percentages in gates represent the frequency of T_{FH} cells within CD4$^+$ T cells and GC B cells within B220$^+$ B cells, respectively. (B) Bar diagrams show relative (top) and absolute cell numbers (bottom) of T_{FH} and GC cells in LNs of mice immunized 14 d earlier with NP-CGG (mean ± SD of 4–5 animals per group). (C) Total (NP_{23}-binding) and high-affinity (NP_4-binding) NP-specific IgG1 antibody levels were measured by ELISA in the sera of control, DL1$^{\Delta/\Delta Ccl19}$, DL4$^{\Delta/\Delta Ccl19}$, and DL1$\Delta^{\Delta/\Delta}$DL4$^{\Delta/\Delta Ccl19}$ mice 14 d after immunization (mean ± SD of 4–5 animals per group). (D) Representative FACS profiles of CD4$^+$CXCR5$^+$PD1$^+$ T_{FH} cells (top; pregated on CD4$^+$ cells) and GL7$^+$CD95$^+$ GC B cells (bottom; pregated on B220$^+$ cells) from control and DL4$^{\Delta/\Delta Ccl19}$ mice 21 d after immunization with *S. mansoni* eggs. (E) Bar diagrams represent relative (top) and absolute cell numbers (bottom) of T_{FH} and GC B cells in LNs of *S. mansoni* egg-immunized mice (mean ± SD of 4–5 animals per group). (F) SEA-specific IgG1 antibody levels as measured by ELISA and optical diffraction (OD) in the diluted sera of control and DL4$^{\Delta/\Delta Ccl19}$ mice at day 21 after immunization with *S. mansoni* eggs (mean ± SEM of 4–5 animals per group). *, $P < 0.05$; **, $P < 0.01$; ***, $P < 0.001$. Unpaired Student's *t* test was used to determine significance. Results are a composite of two independent experiments.

types relative to the total LN fraction, the almost complete Ccl19-Cre–mediated loss of DL4 transcripts and of the *DL4* gene was only seen in activated FDC and FRC (Fig. 6, D and E), consistent with the results obtained by surface protein staining (Fig. 6 B).

To further define DL4-expressing cells within activated LN, immunofluorescence microscopy was performed. Strong DL4 protein expression was observed in several cell types within B cell follicles, namely CD35$^+$ FDC and desmin^{high} MRC and BRC which all also express Pdpn (not shown).

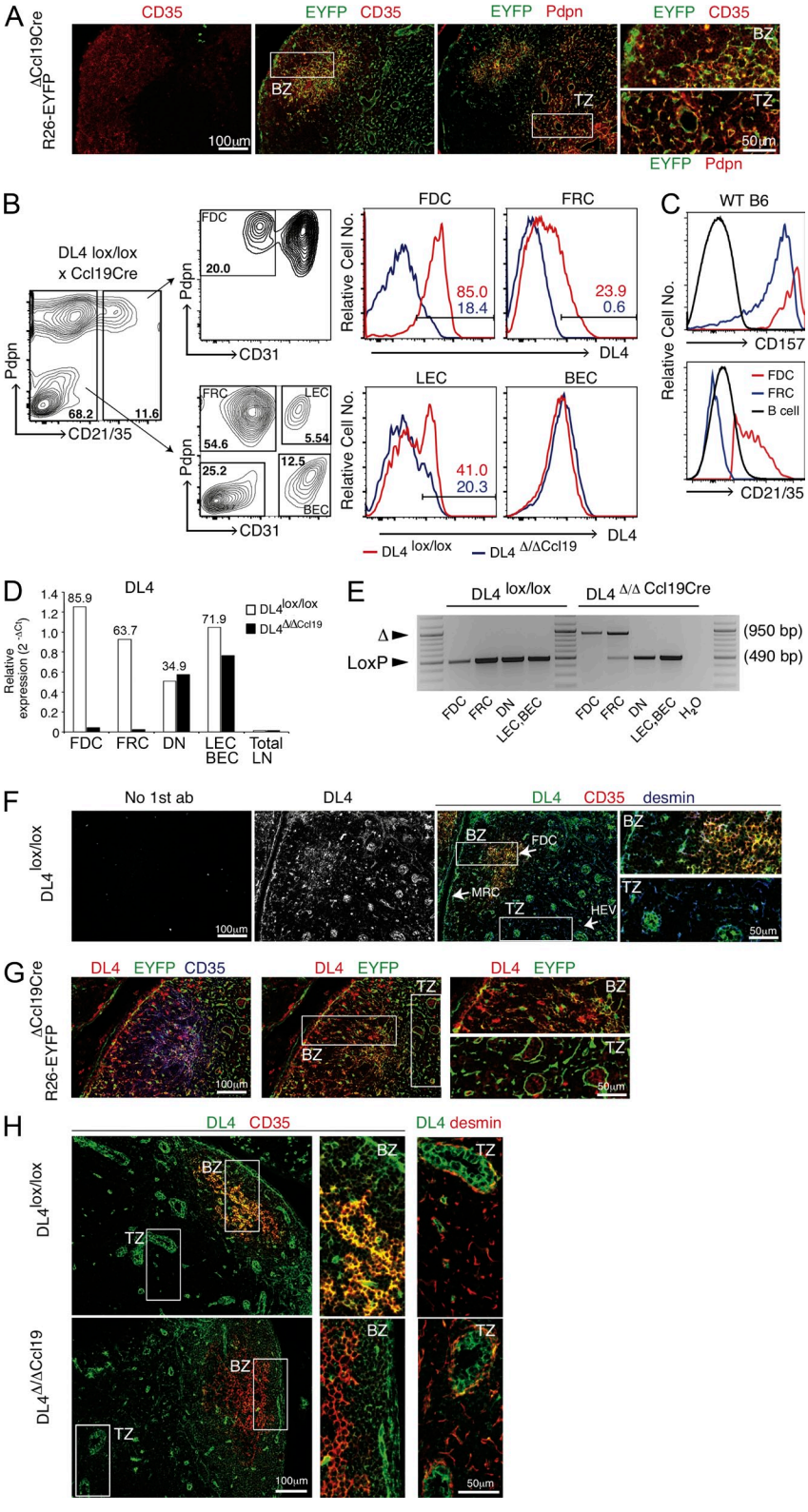

Figure 6. DL4 expression on Ccl19-Cre–expressing follicular fibroblasts regulates Notch-mediated T_{FH} and GC differentiation. (A) LN sections of R26-EYFP$^{\Delta Ccl19}$ mice 5 d after NP-CGG immunization stained for EYFP, CD21/35, and Pdpn expression. EYFP staining reveals Cre recombinase activity through the deletion of the lox-stop-lox cassette in the R26 gene locus. Strong CD21/35 staining in the B zone (BZ) is indicative for activated FDCs and weaker staining for B cells, whereas Pdpn stains FRCs in the T zone (TZ) and activated FDCs in the BZ. White boxes indicate areas of the BZ and TZ, respectively, which are also shown in higher magnification on the right side. (B, left) Representative FACS profiles of LN stromal cells of DL4$^{\Delta/\Delta Ccl19}$ mice 5 d after NP-CGG immunization, gated on Aqua$^-$CD45$^-$Ter119$^-$cells, and further classified as CD35$^+$Pdpn$^+$CD31$^-$ (FDC), CD35$^-$Pdpn$^-$CD31$^-$ (DN), CD35$^-$Pdpn$^+$CD31$^+$ (LEC), or CD35$^-$Pdpn$^-$CD31$^+$ (BEC) stromal cells. Percentages indicate the fraction present in each quadrant or gate. (right) Representative histograms showing DL4 surface expression on FDCs, FRCs, LECs, and BECs, derived from LNs of DL4$^{lox/lox}$ and DL4$^{\Delta/\Delta Ccl19}$ mice. Percentages indicate the proportion of cells expressing DL4 in DL4$^{lox/lox}$ mice (red) versus DL4$^{\Delta/\Delta Ccl19}$ mice (blue). (C) Representative histograms showing CD157 (BP-3) and CD21/35 surface expression on FDC (CD35$^+$Pdpn$^+$CD31$^-$), FRC (CD35$^-$Pdpn$^+$CD31$^-$), and B cells (CD19$^+$TCRβ$^-$). (D) DL4 mRNA expression was assessed for stromal cell subsets (sorted as shown in B) from 6 LNs per mouse derived from DL4$^{lox/lox}$ and DL4$^{\Delta/\Delta Ccl19}$ mice (n = 2) 5 d after NP-CGG immunization. The numbers indicate the fold enrichment relative to the mRNA expression level observed for total LN from DL4$^{lox/lox}$ mice. (E) PCR for the deleted (Δ) versus undeleted (loxP) DL4 gene was performed on DNA from stromal cell subsets (sorted as shown in B) of LNs 5 d after NP-CGG immunization from control and DL4$^{\Delta/\Delta Ccl19}$ mice. (F) LN sections of DL4$^{lox/lox}$ mice 6 d after NP-CGG immunization were stained for DL4, CD21/35, and desmin, as indicated. Arrows indicate different cell types and sites of DL4 expression with BZ and TZ shown on the right in higher magnification. (G) LN sections of R26-EYFP$^{\Delta Ccl19}$ mice 5 d after NP-CGG immunization were stained for DL4, EYFP, and CD21/35, as indicated, with higher magnifications shown on the right. (H) LN sections of DL4$^{lox/lox}$ and DL4$^{\Delta/\Delta Ccl19}$ mice 6 d after NP-CGG immunization were stained for DL4, CD21/35, and desmin, as indicated. Note the loss of DL4 staining in activated CD21/35$^+$ FDCs of DL4$^{\Delta/\Delta Ccl19}$ mice. FDC, follicular DCs; MRCs; BRCs; FRC, T zone fibroblastic reticular cells; HEV, high endothelial venules. Size bars as indicated. Experiments shown are representative of two independent experiments and at least two mice of each genotype.

Within T zones high endothelial venules (HEV) express high levels of DL4 as do scattered single cells, with only weak staining on desmin$^+$ T zone FRC (Fig. 6 F). Therefore, the majority of DL4-expression accessible to T_{FH} cells is found within the follicular fibroblasts: FDC, MRC and BRC. Co-staining of EYFP and DL4 in activated LN of R26-EYFP $^{\Delta Ccl19Cre}$ revealed an overlapping expression mainly in FDC, MRC and BRC (Fig. 6 G). Importantly, histological staining on activated LN of DL4$^{\Delta/\Delta Ccl19}$ mice demonstrated a loss of DL4 expression within MRC and most strikingly within FDC, with DL4 expression on HEV and reticular cells within the T zone being less affected (Fig. 6 H). Collectively, these results strongly suggest that within the LN DL4-expressing FDC, MRC and BRC are likely to function as stromal niche cells for Notch-mediated T_{FH} differentiation.

DISCUSSION

Although Notch signaling has been implicated in various aspects of lymphocyte development and function (Radtke et al., 2013) little is known about the essential ligand-expressing niche cells in SLO that regulate these processes. Here, we present data demonstrating for the first time a functional role of fibroblasts in SLO during Notch-mediated lineage specification and immune responses. Specific DL-expressing reticular fibroblasts function as niche cells to promote the development of MZ B cells and DCs in the spleen and to regulate T_{FH} differentiation in LN and thereby high-affinity antibody generation.

Conditional gene targeting experiments of multiple Notch components revealed that the specification of the MZ B cell fate is strictly dependent on DL1-Notch2 signaling (Saito et al., 2003; Hozumi et al., 2004). However, the identity and splenic localization of DL1-expressing cells driving MZ B cell development remained unknown. Although early studies revealed expression of DL1 in B cells, B cells and their progenitors could be excluded as candidate stimulators of Notch signaling because mice with B cell–specific inactivation of DL1 had normal MZ B cell development (Hozumi et al., 2004). This led to the suggestion that spleen cells other than B cells, probably DCs, might be the essential niche cells for MZ B cell specification. Moreover, this result indicated that DL1-mediated Notch signaling must occur between Notch2-expressing B cell precursor cells and DL1-expressing environmental cells of the spleen rather than between equivalent precursor cells as required for the lateral inhibition model, where fluctuations of Notch signaling between equipotent progenitor cells control developmental cell fate choices (Lewis, 1998).

Although DCs were suggested to be niche cells for MZ B cell development, this hypothesis remained to be tested in vivo. Our results reveal that mice with DC-specific inactivation of DL1 develop normal numbers of MZ B cells, strongly suggesting that DCs do not mediate Notch-induced MZ B cell specification. BECs have also been proposed to be the ligand-expressing cells that drive MZ B cell development, a supposition based on the expression pattern of lacZ knock-in mice and also on the results of BM chimera experiments (Tan et al., 2009). This would be consistent with previous studies showing that endothelial cells are the source of Notch ligands in the developing liver and in the neural stem cell niche (McCright et al., 2002; Shen et al., 2004). However, our inducible genetic LOF data for DL1 in BECs argue against the vasculature being the essential niche for MZ B cell development. In contrast, our results showing that inactivation of DL1 in CD31$^-$Pdpn$^-$DL1$^+$ Ccl19-Cre–expressing fibroblasts results in a dose dependent and complete loss of MZ B cells reveals a novel role for splenic stromal cells in lineage specification of immune cells.

Nonhematopoietic stromal elements of SLO were first described more than 50 years ago (Glegg et al., 1953). For a long time, the primary function of these stromal cells was thought to be mainly structural to maintain the primary architecture of SLOs (Gretz et al., 1997). Only in recent years were stromal cells of SLO phenotypically subdivided into multiple subsets fulfilling distinct and important physiological functions through their cross talk with immune cells (Mueller and Germain, 2009; Turley et al., 2010). One of the major features of SLO is the segregation of B cells and T cells in regionally distinct compartments, B cell follicles, and T cell–rich zones, which are established by two distinct fibroblast cell types and chemokines they produce constitutively. In the B cell zone FDCs express the chemokine CXCL13, thereby attracting B cells expressing the chemokine receptor CXCR5 (Gunn et al., 1998a). The T cell zone is organized by FRCs expressing the chemokines CCL19 and CCL21 (Luther et al., 2000; Link et al., 2007) attracting T lymphocytes and DCs expressing the chemokine receptor CCR7, thereby allowing T cell–DC interactions (Gunn et al., 1998b; Förster et al., 1999; Gunn et al., 1999). Moreover, T zone FRCs have been shown to be an important source of IL-7, which regulates the homeostasis of naive T cells within LNs (Link et al., 2007). More recently, MRCs were defined as phenotypically distinct FRC subset localizing below the marginal sinus in B cell follicles and expressing CXCL13 (Katakai et al., 2008). Interesting new lineage tracing experiments suggest that MRCs are the proliferation-competent precursors of FDCs (Jarjour et al., 2014). The other poorly defined follicular fibroblast type is BRCs, which form a network around CD35$^+$ FDCs and have been lately proposed as a source of oxysterol chemoattractants organizing recently activated B cells in the follicular perimeter around FDC-containing GC (Pereira et al., 2009; Yi et al., 2012; Gatto and Brink, 2013). BRCs are also the likely architects of conduit microchannels transporting small molecules, including antigens and CXCL13, from the marginal sinus to FDCs (Heesters et al., 2014). This incomplete list of diverse functions of reticular fibroblasts shows that they are directly involved in functionally orchestrating immune responses in SLO. Our data extend this list by showing that follicular fibroblasts also regulate important Notch-mediated differentiation processes in spleen and LN.

The current study defines stromal cells (or precursor of these) mediating MZ B cell fate specification as CD31$^-$Pdpn$^-$DL1$^+$

Ccl19-Cre–expressing reticular cells within splenic B cell follicles. As deletion of DL1 expression was visible in MRCs, BRCs, and possibly some FDCs, the critical follicular fibroblast type for MZ B cell fate specification requires further investigation. These findings raise the question of how MZ B cell precursors can receive the essential Notch2 signal if mature MZ B cells mostly localize outside of the marginal sinus that surrounds DL1-expressing B cell follicles. Interestingly, transfer of MZ B cell precursors in vivo showed that they initially localize to the B cell follicle rather than the MZ (Chung et al., 2002). These results may indicate that these precursors need to transit the follicle to fully mature before localizing to the MZ. DL1-expressing follicular fibroblasts may therefore be ideally positioned to provide this maturation signal. But how would mature MZ B cells receive the Notch2 signal, especially given recent evidence that they continuously require Notch2 signals to be retained within the MZ (Simonetti et al., 2013)? Another recent study used intravital microscopy to study MZ and follicular B cell migration within the spleen of living animals (Arnon et al., 2013). This study showed that MZ B cells are very motile and that at least 20% of all MZ B cells shuttle once per hour between the MZ and the follicle. This motility is necessary to rapidly deliver antigens from the open blood stream to secluded follicles. A possible scenario that reconciles the published studies with our data are that MZ B cell progenitors or even mature MZ B cells receive the DL1-mediated Notch2 signal from the follicular fibroblasts while they travel from MZs to follicular zones and back. Once the Notch signals wears off on the MZ B cells, they transiently reposition to the B cell follicle to stay alive or maintain their properties, including their MZ residency. This concept is reminiscent of the one known for naive T cells that recirculate constantly between SLO, lymph, and blood. Naive T cells need to transit in a regular fashion through LN T zones to recognize T zone FRC-derived IL-7 signals to stay alive (Link et al., 2007), besides searching for their cognate antigen. If this concept applies also to MZ B cells, then the follicular fibroblasts may determine the size of the B cell pool found in the neighboring MZ, possibly to keep follicular B cells and MZ B cells in reasonable proportions. Constant cell migration in and out of niches may be a general principle by which the size of a niche-dependent cell population can be controlled.

The development of both MZ B cells and splenic $CD8^{-}CD11b^{+}Esam^{+}$ DCs is mediated via Notch 2 signaling (Saito et al., 2003; Lewis et al., 2011). Because the $Esam^{+}$ DC subset is localized to the same splenic MZ as the MZ B cells (Caton et al., 2007), it was speculated that these lineage decisions might be mediated by the same ligand (Radtke et al., 2013). Indeed, our genetic LOF data obtained via Ccl19-Cre–mediated deletion of DL1 confirm this speculation; DL1 and not DL4 is the critical ligand for the generation of $Esam^{+}$ DCs. Our data also suggest that the same splenic DL1-expressing stromal (precursor) cells might regulate the development of these two distinct immune cell types. Whether DCs show a similar migration pattern as MZ B cells remains to be investigated. Alternatively, DCs might receive a DL1 signal through their interaction with FRC laying outside of the marginal sinus, which showed Ccl19-Cre activity but was undetectable for DL1 expression by immunohistochemistry. $DL1^{\Delta/\Delta Ccl19}$ mice showed also reductions in $CD11b^{+}$ and $CD8^{+}$ DC subsets, which mainly localize to the interfollicular regions and the T zone, respectively. Similar observations were obtained with DC-specific deletion of RBP/J and Notch-2 (Caton et al., 2007; Lewis et al., 2011). It seems plausible that, during their maturation, DCs pass DL1-expressing fibroblasts like MRCs or BRCs, or see such signals during their residence or potential shuttling between the different zones. Again, a role for DL1 expression by T zone FRC or other cells cannot be formally excluded.

Although MZ B cells and splenic DCs are both dependent on DL1-mediated Notch2 signaling, the threshold or sensitivity of Notch signaling for their development or maintenance differs. Our data confirm previous observations that MZ B cell development is dose-dependent in respect to both the ligand (Hozumi et al., 2004) and the receptor (Saito et al., 2003), suggesting that this process is highly sensitive to small changes in receptor or ligand availability. In contrast, the development of splenic DCs, including $Esam^{+}$ DCs, is less sensitive to Notch dosage, as their relative and absolute numbers in $DL1^{+/\Delta Ccl19}$ mutant animals was comparable to control animals. A recent study showed that the development or maintenance of another $CD11b^{+}CD103^{+}$ DC subset present in the lamina propria of the intestine is also dependent on Notch2 signaling (Lewis et al., 2011; Satpathy et al., 2013). Whether this differentiation process is also mediated through the interaction of Notch2-expressing DC progenitors and DL1-expressing fibroblasts within the lamina propria of the intestine is currently unknown and will need further investigation.

In addition to its role in development and possibly lineage specification of immune cells, Notch signaling has also been implicated in regulating peripheral T and B cell responses, in particular through influencing T helper cell functions (Radtke et al., 2013). T_{FH} cells constitute a particular subset of $CD4^{+}$ T cells that provide help for B cells to enhance the generation of germinal centers and high-affinity antibodies. It is currently believed that antigen-presenting cells (including DCs and antigen-specific B cells) activate, and thereby instruct CD4 T cells to differentiate into T_{FH} cells (Crotty, 2011; Ramiscal and Vinuesa, 2013). Recently, we reported that T cell–specific inactivation of both Notch1 and Notch2 results in impaired differentiation of T_{FH} cells in draining LNs of mice injected with T cell–dependent antigens. In accordance with the current view, the absence of functional T_{FH} cells correlated with strongly reduced numbers of GC B cells and high-affinity antibodies (Auderset et al., 2013). Our BM chimera experiments suggest that the cell types mediating Notch-induced T_{FH} differentiation are within the radioresistant compartment. Consistent with this, deletion of DL ligands using Ccl19-Cre indicates that reticular fibroblasts of the B cell follicles are the source of Notch ligands during this process. In this case DL4 (as opposed to DL1) is the essential ligand required.

The Ccl19cre-expressing cells mediating this process are likely to include $CD45^-CD31^-CD35^+Pdpn^+DL4^+$ cells, which phenotypically correspond to activated FDCs. Currently, contributions by $CD35^-Pdpn^+$ MRCs and BRCs cannot be excluded, as they show high DL4 protein expression, loss of transcripts and protein expression in $DL4^{\Delta/\Delta Ccl19}$, and localization in areas of T_{FH} cells. Histological evidence suggests a reduction in DL4 expression within these two follicular stromal cells, but currently there is no well-established flow cytometric analysis protocol allowing a more precise analysis at the single-cell level, including the distinction from T zone FRC that may be a DL4 source undetectable by histological methods. Our results with the mTmG reporter mice also show Ccl19-mediated Cre activity in a small fraction of $CD45^-CD31^+Pdpn^+$ LEC. However, flow cytometric analysis and mRNA expression studies of control and $DL4^{\Delta/\Delta Ccl19}$ mice did only reveal a partial down-regulation of DL4 surface expression in LECs, but not in BECs. In conclusion, the most convincing reduction of DL4 surface expression was observed on activated FDCs that co-localize with T_{FH} cells within B cell follicles. We therefore favor activated FDCs as being the essential niche cells for Notch regulated T_{FH} differentiation.

Although absolute numbers of T_{FH} and GC B cells are significantly reduced, some residual cells are still present. The reason for the presence of these residual cells is currently unknown. It is possible that Jagged ligands might compensate for the loss of DL4 and/or might contribute to T_{FH} differentiation in LN. Alternatively, this might reflect an incomplete inactivation of DL4 in stromal cells of the LN compared with the spleen. Another possibility is that Notch does not instruct T_{FH} differentiation as it does, for example, during thymic T cell lineage specification (Pui et al., 1999; Radtke et al., 1999), but that Notch rather potentiates T_{FH} cell differentiation through the regulation of its genetic program (Helbig et al., 2012). Thus, in the absence of Notch signaling, T_{FH} cells would not be completely lost but their numbers would be reduced. Such a model was very recently put forward to explain how Notch signaling can simultaneously regulate Th1, Th2, and Th17 responses (Bailis et al., 2013). This model unifies contradictory interpretations on the role of Notch signaling in T helper cell differentiation, which were often based on a model in which Notch instructs a particular cell fate at the expense of other lineages. Our results are indeed consistent with a model in which Notch is potentiating or reinforcing T_{FH} cell differentiation. The identity of the Notch ligands and the ligand-expressing cells that induce the development of the other T helper cells (including Th1, Th2, or Th17) in vivo is beyond the scope of this manuscript and needs to be addressed in future studies.

Overall, our findings demonstrate the important contribution of fibroblastic cells in follicles of both the spleen and LN for Notch-mediated differentiation processes and immune reactions. These results, together with the observation that TECs are the ligand-expressing niche cells for Notch-mediated thymopoiesis (Hozumi et al., 2008; Koch et al., 2008), strongly suggest that DL expression on stationary microenvironmental cells represents a generic paradigm. This kind of structural organization allows migrating hematopoietic cells to receive their instructive Notch signals within the correct regional compartments of primary or SLOs.

MATERIALS AND METHODS

Mice. OTII mice and C57BL/6 CD45.1 (B6.SJL-Ptprca/BoyAiTac) were purchased from Charles River and Taconic, respectively. $DL1^{lox/lox}$, $DL4^{lox/lox}$, $J1^{lox/lox}$, and $J2^{lox/lox}$ mice (provided by T. Gridley, Center for Molecular Medicine, Maine Medical Center Research Institute, Scarborough, ME) have already been described and were crossed to MxCre (Hozumi et al., 2004; Mancini et al., 2005; Koch et al., 2008; Xu et al., 2010). DL1lox/lox and DL4lox/lox were also bred with Ccl19-Cre (Chai et al., 2013), PDGFβi-CreERT (T. Petrova, Division of Experimental Oncology 155, CHUV and University of Lausanne, Epalinges, Switzerland; M. Fruttiger, The Lowy Medical Research Institute, La Jolla, CA; Claxton et al., 2008) and CD11c-Cre (Caton et al., 2007). Ccl19-Cre mice were crossed to Gt(ROSA)26Sortm1(EYFP)Cos/J (R26-EYFP) and *Gt(ROSA)26Sor*$^{tm4(ACTB-tdTomato,-EGFP)Luo}$/J (mTmG) mice. Cre-negative littermates were always used as controls. To inactivate the DL1 gene using PDGFβi-CreERT, control and floxed mutant mice were injected i.p. with 1 mg/20 g body weight of tamoxifen (Sigma-Aldrich) for five consecutive days. When using the Mx-Cre system, control and floxed mice received 5 i.p. injections of 2 µg/g body weight polyI-polyC (Invitrogen) at 2-d intervals. All mice on a C57BL/6 background were bred and maintained under pathogen-free conditions and. This study has been reviewed and approved by the Service Vétérinaire Cantonal of Etat de Vaud.

Bone marrow chimeras. BM chimeras were generated using T cell–depleted BM cells from polyI-polyC control and floxed mice. CD45.1 recipient mice were exposed to 2 × 450 rad x-ray-irradiation 24 h before receiving 0.5–1 × 10^7 donor BM cells intravenously. Reverse BM chimeras (all on a CD45.2 background) were generated by transplanting WT CD45.1 BM cells. Radiation chimeras were maintained on antibiotic water (Bactrim®, Roche) for 1 mo. Peripheral blood lymphocytes were isolated according to standard protocols 1 mo after transplantation to analyze BM reconstitution. Cells from the BM were used to assess the deletion efficiency. Primers for the DL1 deletion PCR were DL1Dfwd 5′-CACACCTCCTACTTACCTGA-3′ and DL1Drev 5′-GGCGCTCAAAGGATATGGGA-3′. For DL4 deletion, primers were DL4loxfwd 5′-GTGCTGGGACTGTAGCCACT-3′ and DL4Drev 5′-CTCGTCTGTTCGCCAAATCTTAC-3′.

Immunizations. Mice were either immunized s.c. with 25 µg per site of NP_{35}-CGG (Biosearch technologies) in alum (Sigma) or with 5000 *S. mansoni* eggs (provided by F. Trottein, Institut Pasteur de Lille, Université Lille Nord de France, Lille, France). Draining LNs were isolated 14 and 21 d after injection, respectively.

Isolation of cells. Draining axillary, brachial and inguinal LNs were dissected, cut into small pieces and digested for 30 min at 37°C in DMEM (GIBCO BRL Life Technologies) containing additional $CaCl_2$ (1.2M), 2% (vol/vol) FCS, type IV collagenase (3 µg/ml; Worthington), DNase (40 µg/ml; Roche); with shaking and some pipetting. For isolation of spleen stromal cells, 1ml of the above digestion mix was injected into spleen before cutting it into small pieces and digesting it as LNs. For isolation of splenic DCs, spleen was digested in the buffer indicated above but using collagenase D (Roche; 1 mg/ml) and digesting for 20 min. After enzymatic digestion, cell suspensions were passed through a 40-µm gauze filter and washed with PBS containing 5% FCS and 5 mM EDTA (Sigma). To further enrich the splenic stromal cell fraction, red blood cells were lysed for 1 min using ammonium chloride, and hematopoietic cells depleted using two sequential rounds of panning on Ab-coated plates coated with anti-CD45 (clone M1/9.4.3).

Flow cytometry. Non-specific staining was blocked using anti-FcR antibodies (2.4.G2). The following mAbs conjugates were used: CD4 (Clone GK1.5), CD8 (YTS109.4), B220 (RA3-6B2), CD21 (ebio8D9), CD23

(B3B4), CD1d (1B1), PD-1 (J43), GL-7, CD95 (15A7), Gr1 (RB6-8C5), Ter119 (TER-119), CD11c (N418), CD11b (M1/70), MHCII (M5/114.15.2), Esam (1G8), CD45.1 (A20), CD45.2 (104), F4/80 (BM8), were purchased from eBioscience, BD, or BioLegend. Antibodies to CD21/35 (7E9), CD31 (390), Pdpn (8.1.1), pan-CD45 (30F11) and CD157 (BP-3.4) were grown and coupled in-house. Purified CXCR5 was used in combination with goat anti-rat IgG-FITC (Invitrogen). Biotinylated antibodies were revealed with streptavidin conjugates. Antibodies to DL1 (30B11.1) and DL4 (9A1.5) were developed and biotinylated in-house (Fiorini et al., 2008) and DL4 stainings were done using PBS/2% FCS in the absence of any EDTA. Dead cell exclusion was achieved using 7-AAD, DAPI or live/dead fixable aqua fluorescent reactive dye (Invitrogen). Analyses were performed on Cyan ADP (Dako) or LSRII (Becton Dickinson) flow cytometers and data processed with FlowJo (Tree Star). Cell sorting was performed on a FACS Aria II (BD Bioscience).

Immunohistochemistry. Cryostat sections (8–10 µm) of Tissue-Tek OCT (Sakura)-embedded LN or spleen were collected on Superfrost/Plus glass slides (Thermo Fisher Scientific), and then air dried overnight, fixed in ice-cold acetone for 10 min, and rehydrated in PBS. Sections were blocked using 0.1% BSA and 1–4% animal serum in PBS, followed by a streptavidin-biotin blocking kit (Vector Laboratories). Sections were quenched with 0.3% H_2O_2 in PBS, if tyramide amplification was used. The primary antibody labelings were performed for 60 min or overnight at room temperature using the following antibodies: CD4 (clone H129), B220 (RA3-6B2), CD35 (8C12), Pdpn (8.1.1), DL1 (30B11), MAdCAM-1 (Meca-89), rat anti-IgM (Invitrogen), rabbit anti-laminin (Sigma-Aldrich), rabbit anti-desmin (ProGen), sheep anti-IgD (The Binding Site), goat anti-collagen IV (Southern Biotech), and goat anti-DL4 (AF1389; R&D systems). Secondary antibodies used were: donkey anti–rat biotin, donkey anti–rat Cy3, donkey anti–rabbit Cy3, donkey anti–sheep APC (all from Jackson ImmunoResearch Laboratories), streptavidin Alexa Fluor 488, donkey anti–rabbit Alexa Fluor 647 (both from Invitrogen). For DL1 and DL4 labeling, primary antibodies were detected using a biotinylated donkey anti–goat IgG followed by HRP-coupled streptavidin (both from Jackson ImmunoResearch Laboratories) and tyramide Signal Amplification (Invitrogen) according to the manufacturer's instructions, but using a borate buffer (0.1 M in PBS, pH 8.5) for tyramide dilution. To visualize endogenous GFP or EYFP, LN and spleen were fixed in 1% PFA at 4°C for 2 h, and then saturated in 30% sucrose in PBS overnight at 4°C before embedding in OCT and freezing in an ethanol dry ice bath. GFP was detected using a rabbit anti-GFP antibody followed by Alexa Fluor 488–conjugated donkey anti–rabbit IgG (both from Invitrogen). Images were acquired on an AxioImager.Z1 microscope with an AxioCam MRM camera (Carl Zeiss) and treated using Adobe Photoshop.

Serum antibody quantification. Antigen-specific IgG1 antibodies in sera were quantified by antigen-capture ELISAs, detected with biotinylated goat anti–mouse IgG1. Total or high-affinity NP-specific IgG1 antibodies levels were measured by ELISA using NP_{23}-BSA or NP_4-BSA (Biosearch Technologies). *S. mansoni*–specific IgG1 were measured by ELISA using *S. mansoni*–soluble egg antigens (SEA).

Quantitative real-time PCR. Total RNA was extracted from different stromal cell populations sorted from spleen or LN using the TRIZOL reagent (Invitrogen). RNA was reverse-transcribed using the Superscript II reverse transcription kit (Invitrogen) and real-time PCR reactions were performed using SYBR Green and a 7900 HT Fast Real-Time PCR System (both from Applied Biosystems) for 40 cycles. Values were normalized to HPRT ($2^{-\Delta CT}$). Primer sequences were as follows: DL1fwd, 5′-GCACTACTACGGAGAAGGTTGCTC-3′; DL1rev, 5′-TCACACCCTGGCAGACAGATTG-3′; DL4fwd, 5′-CCTCTCGAACTTGGACTTGC-3′; DL4rev, 5′-GCTCCTGCTTAATGCCAAAC-3′; Pdpnfwd, 5′-ACAACCACAGGTGCTACTGGAG-3′; Pdpnrev, 5′-GTTGCTGAGGTGGACAGTTCCT-3′; HPRTfwd, 5′-GTTGGATACAGGCCAGACTTTGTTG-3′; HPRTrev, 5′-GATTCAACTTGCGCTCATCTTAGGC-3′.

Deletion PCR on genomic DNA isolated from stromal subsets. Genomic DNA was isolated from sorted stromal subsets (FDCs, FRCs, LECs, BECs, and DN). PCRs were performed to determine deletion efficiency of loxP targeted alleles of DL1 (splenic stromal subsets) or DL4 (LN stromal subsets). The deleted and undeleted lox alleles were detected separately by PCR using specific primers.

DL1 deletion PCR primer sequences were as follows: DL1lox_sense, 5′-CACACCTCCTACTTACCTGA-3′; DL1lox_as, 5′-GAGAGTACTGGATGGAGCAAG-3′; DL13'lox Del, 5′-GGCGCTCAAAGGATATGGGA-3′. The triple PCR will amplify a 238-bp fragment of the floxed allele and a 337-bp deletion fragment.

DL4 deletion PCR primer sequences were as follows: DL4lox_sense, 5′-GTGCTGGGACTGTAGCCACT-3′; DL4lox_as, 5′-TGTTAGGGATGTCGCTCTCC-3′; DL43'lox Del, 5′-CTCGTCTGTTCGCCAAATCTTAC-3′. The triple PCR will amplify a 490-bp fragment of the floxed allele and a 950-bp deletion fragment.

T cell proliferation assay. Splenic and LN $CD4^+$ T cells from OVA-specific OT-II transgenic mice were enriched using MACS beads. After staining with 5 µM CFSE, cells were injected i.v. ($1–3 \times 10^6$ per animal) into $DL1^{lox/lox}$ Ccl19-Cre or control mice. After 24 h, recipient mice received 100 µg OVA and 75 µg LPS i.v. (both from Sigma-Aldrich) and were analyzed 3 or 5 d later.

Statistical analysis. Bar diagrams were compiled using Graph Pad Prism or Excel statistical analysis software. For comparison of pooled data between two different groups, unpaired Student's *t* tests were used to determine significance. *, $P < 0.05$; **, $P < 0.01$.

Ethics statement. All animal work was conducted according to Swiss national guidelines. All mice were kept in the animal facility under EPFL or UNIL animal care regulations. They were housed in individual cages at 23 ± 1°C with a 12-h light/dark cycle. All animals were supplied with food and water ad libitum. This study has been reviewed and approved by the Service Vétérinaire Cantonal of Etat de Vaud.

We thank Tatiana Petrova and Markus Fruttiger for the PDGFβi-CreERT mice, Tom Gridley for the floxed Jagged2 mice, and François Trottein for *Schistosoma* eggs. We would like to acknowledge Olivier Randin, Marianne Nkosi, Christelle Dubey and Karin Schäuble for technical assistance, the Flow Cytometry Core Facility of the EPFL and UNIL for cell sorting, and the UNIL Histology Core for making cryosections.

This work was supported in part by the Swiss National Science Foundation (to F. Radtke, F. Tacchini-Cottier, and S.A. Luther), the Swiss Cancer League (to F. Radtke) and the Taiwan National Science Council (to H.-Y. Huang).

The authors declare no competing financial interests.

Submitted: 6 December 2013
Accepted: 15 September 2014

REFERENCES

Arnon, T.I., R.M. Horton, I.L. Grigorova, and J.G. Cyster. 2013. Visualization of splenic marginal zone B-cell shuttling and follicular B-cell egress. *Nature*. 493:684–688. http://dx.doi.org/10.1038/nature11738

Auderset, F., S. Schuster, N. Fasnacht, M. Coutaz, M. Charmoy, U. Koch, S. Favre, A. Wilson, F. Trottein, J. Alexander, et al. 2013. Notch signaling regulates follicular helper T cell differentiation. *J. Immunol.* 191:2344–2350. http://dx.doi.org/10.4049/jimmunol.1300643

Bailis, W., Y. Yashiro-Ohtani, T.C. Fang, R.D. Hatton, C.T. Weaver, D. Artis, and W.S. Pear. 2013. Notch simultaneously orchestrates multiple helper T cell programs independently of cytokine signals. *Immunity*. 39:148–159. http://dx.doi.org/10.1016/j.immuni.2013.07.006

Caton, M.L., M.R. Smith-Raska, and B. Reizis. 2007. Notch-RBP-J signaling controls the homeostasis of CD8- dendritic cells in the spleen. *J. Exp. Med.* 204:1653–1664.

Chai, Q., L. Onder, E. Scandella, C. Gil-Cruz, C. Perez-Shibayama, J. Cupovic, R. Danuser, T. Sparwasser, S.A. Luther, V. Thiel, et al. 2013.

Maturation of lymph node fibroblastic reticular cells from myofibroblastic precursors is critical for antiviral immunity. *Immunity*. 38:1013–1024. http://dx.doi.org/10.1016/j.immuni.2013.03.012

Chung, J.B., R.A. Sater, M.L. Fields, J. Erikson, and J.G. Monroe. 2002. CD23 defines two distinct subsets of immature B cells which differ in their responses to T cell help signals. *Int. Immunol.* 14:157–166. http://dx.doi.org/10.1093/intimm/14.2.157

Claxton, S., V. Kostourou, S. Jadeja, P. Chambon, K. Hodivala-Dilke, and M. Fruttiger. 2008. Efficient, inducible Cre-recombinase activation in vascular endothelium. *Genesis*. 46:74–80. http://dx.doi.org/10.1002/dvg.20367

Crotty, S. 2011. Follicular helper CD4 T cells (TFH). *Annu. Rev. Immunol.* 29:621–663. http://dx.doi.org/10.1146/annurev-immunol-031210-101400

Fiorini, E., I. Ferrero, E. Merck, S. Favre, M. Pierres, S.A. Luther, and H.R. MacDonald. 2008. Cutting edge: thymic crosstalk regulates delta-like 4 expression on cortical epithelial cells. *J. Immunol.* 181:8199–8203. http://dx.doi.org/10.4049/jimmunol.181.12.8199

Förster, R., A. Schubel, D. Breitfeld, E. Kremmer, I. Renner-Müller, E. Wolf, and M. Lipp. 1999. CCR7 coordinates the primary immune response by establishing functional microenvironments in secondary lymphoid organs. *Cell*. 99:23–33. http://dx.doi.org/10.1016/S0092-8674(00)80059-8

Gatto, D., and R. Brink. 2013. B cell localization: regulation by EBI2 and its oxysterol ligand. *Trends Immunol.* 34:336–341. http://dx.doi.org/10.1016/j.it.2013.01.007

Glegg, R.E., D. Eidinger, and C.P. Leblond. 1953. Some carbohydrate components of reticular fibers. *Science*. 118:614–616. http://dx.doi.org/10.1126/science.118.3073.614

Gretz, J.E., A.O. Anderson, and S. Shaw. 1997. Cords, channels, corridors and conduits: critical architectural elements facilitating cell interactions in the lymph node cortex. *Immunol. Rev.* 156:11–24. http://dx.doi.org/10.1111/j.1600-065X.1997.tb00955.x

Gunn, M.D., V.N. Ngo, K.M. Ansel, E.H. Ekland, J.G. Cyster, and L.T. Williams. 1998a. A B-cell-homing chemokine made in lymphoid follicles activates Burkitt's lymphoma receptor-1. *Nature*. 391:799–803. http://dx.doi.org/10.1038/35876

Gunn, M.D., K. Tangemann, C. Tam, J.G. Cyster, S.D. Rosen, and L.T. Williams. 1998b. A chemokine expressed in lymphoid high endothelial venules promotes the adhesion and chemotaxis of naive T lymphocytes. *Proc. Natl. Acad. Sci. USA*. 95:258–263. http://dx.doi.org/10.1073/pnas.95.1.258

Gunn, M.D., S. Kyuwa, C. Tam, T. Kakiuchi, A. Matsuzawa, L.T. Williams, and H. Nakano. 1999. Mice lacking expression of secondary lymphoid organ chemokine have defects in lymphocyte homing and dendritic cell localization. *J. Exp. Med.* 189:451–460. http://dx.doi.org/10.1084/jem.189.3.451

Heesters, B.A., R.C. Myers, and M.C. Carroll. 2014. Follicular dendritic cells: dynamic antigen libraries. *Nat. Rev. Immunol.* 14:495–504. http://dx.doi.org/10.1038/nri3689

Helbig, C., R. Gentek, R.A. Backer, Y. de Souza, I.A. Derks, E. Eldering, K. Wagner, D. Jankovic, T. Gridley, P.D. Moerland, et al. 2012. Notch controls the magnitude of T helper cell responses by promoting cellular longevity. *Proc. Natl. Acad. Sci. USA*. 109:9041–9046. http://dx.doi.org/10.1073/pnas.1206044109

Hozumi, K., N. Negishi, D. Suzuki, N. Abe, Y. Sotomaru, N. Tamaoki, C. Mailhos, D. Ish-Horowicz, S. Habu, and M.J. Owen. 2004. Delta-like 1 is necessary for the generation of marginal zone B cells but not T cells in vivo. *Nat. Immunol.* 5:638–644. http://dx.doi.org/10.1038/ni1075

Hozumi, K., C. Mailhos, N. Negishi, K. Hirano, T. Yahata, K. Ando, S. Zuklys, G.A. Holländer, D.T. Shima, and S. Habu. 2008. Delta-like 4 is indispensable in thymic environment specific for T cell development. *J. Exp. Med.* 205:2507–2513. http://dx.doi.org/10.1084/jem.20080134

Jarjour, M., A. Jorquera, I. Mondor, S. Wienert, P. Narang, M.C. Coles, F. Klauschen, and M. Bajénoff. 2014. Fate mapping reveals origin and dynamics of lymph node follicular dendritic cells. *J. Exp. Med.* 211:1109–1122. http://dx.doi.org/10.1084/jem.20132409

Junt, T., E. Scandella, and B. Ludewig. 2008. Form follows function: lymphoid tissue microarchitecture in antimicrobial immune defence. *Nat. Rev. Immunol.* 8:764–775. http://dx.doi.org/10.1038/nri2414

Katakai, T., H. Suto, M. Sugai, H. Gonda, A. Togawa, S. Suematsu, Y. Ebisuno, K. Katagiri, T. Kinashi, and A. Shimizu. 2008. Organizer-like reticular stromal cell layer common to adult secondary lymphoid organs. *J. Immunol.* 181:6189–6200. http://dx.doi.org/10.4049/jimmunol.181.9.6189

Koch, U., E. Fiorini, R. Benedito, V. Besseyrias, K. Schuster-Gossler, M. Pierres, N.R. Manley, A. Duarte, H.R. Macdonald, and F. Radtke. 2008. Delta-like 4 is the essential, nonredundant ligand for Notch1 during thymic T cell lineage commitment. *J. Exp. Med.* 205:2515–2523. http://dx.doi.org/10.1084/jem.20080829

Lewis, J. 1998. Notch signalling and the control of cell fate choices in vertebrates. *Semin. Cell Dev. Biol.* 9:583–589. http://dx.doi.org/10.1006/scdb.1998.0266

Lewis, K.L., M.L. Caton, M. Bogunovic, M. Greter, L.T. Grajkowska, D. Ng, A. Klinakis, I.F. Charo, S. Jung, J.L. Gommerman, et al. 2011. Notch2 receptor signaling controls functional differentiation of dendritic cells in the spleen and intestine. *Immunity*. 35:780–791. http://dx.doi.org/10.1016/j.immuni.2011.08.013

Link, A., T.K. Vogt, S. Favre, M.R. Britschgi, H. Acha-Orbea, B. Hinz, J.G. Cyster, and S.A. Luther. 2007. Fibroblastic reticular cells in lymph nodes regulate the homeostasis of naive T cells. *Nat. Immunol.* 8:1255–1265. http://dx.doi.org/10.1038/ni1513

Luther, S.A., H.L. Tang, P.L. Hyman, A.G. Farr, and J.G. Cyster. 2000. Coexpression of the chemokines ELC and SLC by T zone stromal cells and deletion of the ELC gene in the plt/plt mouse. *Proc. Natl. Acad. Sci. USA*. 97:12694–12699. http://dx.doi.org/10.1073/pnas.97.23.12694

Mancini, S.J., N. Mantei, A. Dumortier, U. Suter, H.R. MacDonald, and F. Radtke. 2005. Jagged1-dependent Notch signaling is dispensable for hematopoietic stem cell self-renewal and differentiation. *Blood*. 105:2340–2342. http://dx.doi.org/10.1182/blood-2004-08-3207

McCright, B., J. Lozier, and T. Gridley. 2002. A mouse model of Alagille syndrome: Notch2 as a genetic modifier of Jag1 haploinsufficiency. *Development*. 129:1075–1082.

Mueller, S.N., and R.N. Germain. 2009. Stromal cell contributions to the homeostasis and functionality of the immune system. *Nat. Rev. Immunol.* 9:618–629.

Onder, L., E. Scandella, Q. Chai, S. Firner, C.T. Mayer, T. Sparwasser, V. Thiel, T. Rülicke, and B. Ludewig. 2011. A novel bacterial artificial chromosome-transgenic podoplanin-cre mouse targets lymphoid organ stromal cells in vivo. *Front. Immunol.* 2:50. http://dx.doi.org/10.3389/fimmu.2011.00050

Pereira, J.P., L.M. Kelly, Y. Xu, and J.G. Cyster. 2009. EBI2 mediates B cell segregation between the outer and centre follicle. *Nature*. 460:1122–1126.

Pui, J.C., D. Allman, L. Xu, S. DeRocco, F.G. Karnell, S. Bakkour, J.Y. Lee, T. Kadesch, R.R. Hardy, J.C. Aster, and W.S. Pear. 1999. Notch1 expression in early lymphopoiesis influences B versus T lineage determination. *Immunity*. 11:299–308. http://dx.doi.org/10.1016/S1074-7613(00)80105-3

Radtke, F., A. Wilson, G. Stark, M. Bauer, J. van Meerwijk, H.R. MacDonald, and M. Aguet. 1999. Deficient T cell fate specification in mice with an induced inactivation of Notch1. *Immunity*. 10:547–558. http://dx.doi.org/10.1016/S1074-7613(00)80054-0

Radtke, F., H.R. MacDonald, and F. Tacchini-Cottier. 2013. Regulation of innate and adaptive immunity by Notch. *Nat. Rev. Immunol.* 13:427–437. http://dx.doi.org/10.1038/nri3445

Ramiscal, R.R., and C.G. Vinuesa. 2013. T-cell subsets in the germinal center. *Immunol. Rev.* 252:146–155. http://dx.doi.org/10.1111/imr.12031

Saito, T., S. Chiba, M. Ichikawa, A. Kunisato, T. Asai, K. Shimizu, T. Yamaguchi, G. Yamamoto, S. Seo, K. Kumano, et al. 2003. Notch2 is preferentially expressed in mature B cells and indispensable for marginal zone B lineage development. *Immunity*. 18:675–685. http://dx.doi.org/10.1016/S1074-7613(03)00111-0

Satpathy, A.T., C.G. Briseño, J.S. Lee, D. Ng, N.A. Manieri, W. Kc, X. Wu, S.R. Thomas, W.L. Lee, M. Turkoz, et al. 2013. Notch2-dependent classical dendritic cells orchestrate intestinal immunity to attaching-and-effacing bacterial pathogens. *Nat. Immunol.* 14:937–948. http://dx.doi.org/10.1038/ni.2679

Sekine, C., Y. Moriyama, A. Koyanagi, N. Koyama, H. Ogata, K. Okumura, and H. Yagita. 2009. Differential regulation of splenic CD8- dendritic cells and marginal zone B cells by Notch ligands. *Int. Immunol.* 21:295–301. http://dx.doi.org/10.1093/intimm/dxn148

Shen, Q., S.K. Goderie, L. Jin, N. Karanth, Y. Sun, N. Abramova, P. Vincent, K. Pumiglia, and S. Temple. 2004. Endothelial cells stimulate self-renewal and expand neurogenesis of neural stem cells. *Science*. 304:1338–1340. http://dx.doi.org/10.1126/science.1095505

Sheng, Y., T. Yahata, N. Negishi, Y. Nakano, S. Habu, K. Hozumi, and K. Ando. 2008. Expression of Delta-like 1 in the splenic non-hematopoietic cells is essential for marginal zone B cell development. *Immunol. Lett.* 121:33–37. http://dx.doi.org/10.1016/j.imlet.2008.08.001

Simonetti, G., A. Carette, K. Silva, H. Wang, N.S. De Silva, N. Heise, C.W. Siebel, M.J. Shlomchik, and U. Klein. 2013. IRF4 controls the positioning of mature B cells in the lymphoid microenvironments by regulating NOTCH2 expression and activity. *J. Exp. Med.* 210:2887–2902. http://dx.doi.org/10.1084/jem.20131026

Skokos, D., and M.C. Nussenzweig. 2007. CD8- DCs induce IL-12-independent Th1 differentiation through Delta 4 Notch-like ligand in response to bacterial LPS. *J. Exp. Med.* 204:1525–1531.

Tan, J.B., K. Xu, K. Cretegny, I. Visan, J.S. Yuan, S.E. Egan, and C.J. Guidos. 2009. Lunatic and manic fringe cooperatively enhance marginal zone B cell precursor competition for delta-like 1 in splenic endothelial niches. *Immunity*. 30:254–263. http://dx.doi.org/10.1016/j.immuni.2008.12.016

Turley, S.J., A.L. Fletcher, and K.G. Elpek. 2010. The stromal and haematopoietic antigen-presenting cells that reside in secondary lymphoid organs. *Nat. Rev. Immunol.* 10:813–825. http://dx.doi.org/10.1038/nri2886

Xu, J., L.T. Krebs, and T. Gridley. 2010. Generation of mice with a conditional null allele of the Jagged2 gene. *Genesis*. 48:390–393. http://dx.doi.org/10.1002/dvg.20626

Yi, T., X. Wang, L.M. Kelly, J. An, Y. Xu, A.W. Sailer, J.A. Gustafsson, D.W. Russell, and J.G. Cyster. 2012. Oxysterol gradient generation by lymphoid stromal cells guides activated B cell movement during humoral responses. *Immunity*. 37:535–548. http://dx.doi.org/10.1016/j.immuni.2012.06.015

Yuan, J.S., P.C. Kousis, S. Suliman, I. Visan, and C.J. Guidos. 2010. Functions of notch signaling in the immune system: consensus and controversies. *Annu. Rev. Immunol.* 28:343–365. http://dx.doi.org/10.1146/annurev.immunol.021908.132719